ESTIMATION OF SIDEFORCE AND YAWING MOMENT DERIVATIVES DUE TO SIDESLIP FOR COMPLETE AIRCRAFT AT SUBSONIC SPEEDS

1. NOTATION AND UNITS

The derivative notation used is that proposed in ARC R&M 3562 (Hopkin, 1970) and described in Item No. 86021. Coefficients and aeronormalised derivatives are evaluated in aerodynamic body axes with origin at the aircraft centre of gravity and with the wing span as the characteristic length. The derivatives Y_v and N_v are often written as $\partial C_Y/\partial\beta$ and $\partial C_n/\partial\beta$ or $C_{Y\beta}$ and $C_{n\beta}$ in other systems of notation, but attention must be paid to the reference dimensions used and it is to be noted that a constant datum value of V is employed in the Hopkin system.

This Item makes use of several other Items which have been produced at different times over a period of many years. Although the nomenclature in these Items is consistent for the important parameters such as stability derivatives, it involves some variation and duplication for the less significant parameters. Because of this, and to avoid repetition, the Notation given here is limited to the major quantities appearing in the main text of this Item and to quantities not appearing in other Items. When referred to the method in another Item the user should consult the Notation at the front of that particular Item before carrying out any calculations.

The computer program ESDUpac A0025 associated with Item No. 00025, calculates the stability derivatives treated in this Item.

1.1 Notation

		SI	*British*
b	wing span	m	ft
C_L	lift coefficient $L/\frac{1}{2}\rho V^2 S$		
C_n	yawing moment coefficient, $\mathcal{N}/\frac{1}{2}\rho V^2 Sb$		
C_Y	sideforce coefficient, $Y/\frac{1}{2}\rho V^2 S$		
L	lift	N	lbf
$\mathcal{N}$	yawing moment	N m	lbf ft
N_v	yawing moment derivative due to sideslip, $N_v = (\partial\mathcal{N}/\partial v)/\frac{1}{2}\rho VSb$		
S	wing planform area	m^2	ft^2
V	velocity of aircraft relative to air	m/s	ft/s
v	sideslip velocity	m/s	ft/s
Y	sideforce	N	lbf
Y_v	sideforce derivative due to sideslip, $Y_v = (\partial Y/\partial v)/\frac{1}{2}\rho VS$		

Issued September 1982
With Amendments A and B, October 2000 – 23 pages
This page Amendment B

α	angle of attack of longitudinal body axis (see definition of reference axis in Section 1.2)	degree	degree
α_w	angle between wing zero-lift line and longitudinal body axis, so that angle of attack of wing zero-lift line is $\alpha + \alpha_w$ (see definition of reference axis in Section 1.2)	degree	degree
β	sideslip angle, $\sin^{-1}(v/V)$	radian	radian

Additional Symbols

$(\ )_F$	denotes component due to fin (or fin and undeflected rudder), allowing for presence of body, wing and tailplane
$(\ )_f$	denotes component due to deployment of trailing-edge flaps
$(\ )_n$	denotes component due to nacelles
$(\ )_{WB}$	denotes component due to wing-body combination

1.2 Longitudinal Body Reference Axis

The angle of attack of the body may be expressed in terms of any longitudinal axis which lies in the aircraft plane of symmetry and is fixed in the body, provided that the same axis is used in all calculations. Because the stability derivatives are defined in terms of a set of aerodynamic body axes with their origin at the aircraft centre of gravity (moment reference centre) the calculation of the fin contribution is considerably simplified if a body reference axis which passes through the aircraft centre of gravity is chosen. Aircraft dimensions are customarily defined with respect to some geometrically convenient "horizontal datum" axis which lies in the aircraft plane of symmetry and is fixed in the body but which does not necessarily pass through the centre of gravity position. Therefore, in practice, the best longitudinal body axis to choose for calculation purposes is one which is parallel to the "horizontal datum" axis but which is displaced vertically so as to pass through the centre of gravity position. Such a reference axis is assumed in this Item.

2. INTRODUCTION

The sideforce and yawing moment derivatives due to sideslip, Y_v and N_v, of an aircraft are customarily estimated by calculating the effects of the major components of the aircraft separately and adding together the part derivatives so obtained. This Item demonstrates how to combine the Data Items dealing with the major components and illustrates the overall accuracy of prediction by comparison with wind-tunnel data for complete aircraft models. It should be noted that the methods in the various Data Items are applicable over the range of aircraft incidences for which there is a linear variation of sideforce and yawing moment coefficients with angle of sideslip and of lift coefficient with angle of attack. They apply at subsonic speeds, for Mach numbers below that at which the aerodynamic characteristics start to diverge rapidly with Mach number.

The major contributions to Y_v and N_v and the Data Items from which they may be estimated are listed in Table 2.1. The Items dealing specifically with Y_v and N_v will often require the introduction of additional information from Items of a more general nature. These are also identified in Table 2.1. Comparisons between the total values of Y_v and N_v predicted by the Data Item methods and wind-tunnel data, for a variety of different types of aircraft, are discussed in Section 3. The Derivation and Reference are given

in Section 4. Section 5 contains a detailed worked example which demonstrates the calculation of the various components of Y_v and N_v for a particular aircraft for both the cruise (clean) configuration and the landing configuration. The example devotes a separate subsection to the calculation of each component of Y_v and N_v and describes at which stages in the calculation the additional Data Items listed in Table 2.1 may be needed to complement those dealing specifically with Y_v and N_v. It also provides guidance and information on particular points which are not covered in other Data Items. It is therefore useful to refer to the appropriate subsection in the example when each Data Item dealing with the separate components of Y_v and N_v is used.

TABLE 2.1

*Component**	*Due to*	*Calculated from Item No.*	*Possible additional Item Nos*
$(Y_v)_{WB}$ $(N_v)_{WB}$	wing-body combination	79006[18]	76003[17]
$(Y_v)_n$ $(N_v)_n$	nacelles	79006[18]	–
$(Y_v)_F$ $(N_v)_F$	fin sideforce (in presence of body, wing and tailplane), rudder undeflected	82010[20] Aero C.01.01.01[8] Aero C.01.01.02[9]	70011[11]
$(Y_v)_f$ $(N_v)_f$	trailing-edge flap deployment	81013[19]	Aero C.01.01.01[8] Aero F.01.01.08[5] and 09[4] Aero F.02.01.06[2] and 07[1] Aero W.01.01.01[6] and 05[7] 66032[10] 70011[11] 74009[12], 10[13], 11[14] and 12[15] 75013[16] 76003[17] 82010[20] 87024[47]

* Item No. Aero A.07.01.00[3] gives a brief introduction to the various components of the yawing-moment stability derivatives and their related Data Items.

(Derivation numbers are given as indices.)

The total values of Y_v and N_v for an aircraft are obtained by evaluating each of the components in Table 2.1, *for the same angle of attack*, and summing the results. This is usually sufficient for providing initial estimates. (It may be noted that no direct contribution is estimated for the tailplane, which is assumed to influence Y_v and N_v only through its effect on the magnitude and centre of pressure position of the fin sideforce, see Section 3.2.2.)

3. COMPARISONS WITH EXPERIMENTAL DATA

The accuracy with which the methods in the Data Items listed in Section 2 predict Y_v and N_v for complete aircraft has been assessed by making comparisons with the values measured in the wind-tunnel tests reported in Derivations 21 to 45 (Section 4.1). Data have been studied for a wide variety of different aircraft models representing civil transport aircraft, high performance fighter aircraft and light and general aviation aircraft, and also for many simpler wind-tunnel models employed to examine the effect of systematic variations of geometric parameters. The great majority of these data have been taken from low-speed tests but a limited number of results from tests at high subsonic speeds (Mach number ≈ 0.8) have also been considered. Comparisons of predicted and experimental values have been made for the cruise (clean) configuration and, when available, for configurations with trailing-edge flaps deployed as for landing or take-off.

It should be noted that the experimental derivatives are defined on the usually reliable assumption that the sideforce and yawing moment coefficients vary linearly with the angle of sideslip for a small range of sideslip angles about zero (typically $|\beta| \leq 2°$ or $|\beta| \leq 5°$). The Data Item methods predict values which are consistent with this definition of the derivatives. As the angle of sideslip increases the experimental sideforce and yawing moment coefficients eventually diverge from the linear variation. The extent of the divergence and the point at which it becomes significant vary from aircraft to aircraft but it is usually apparent at $\beta = 10°$, with high-wing aircraft tending to show an earlier divergence than low-wing aircraft. The Data Item methods make no attempt to predict these variations.

3.1 Variation with α and C_L

The predicted values of Y_v and N_v are almost constant with angle of attack and lift coefficient (see Example, Section 5), and in this respect they are in agreement with the experimental trends, although the latter occasionally show fluctuations and variations which are not predicted. These variations in the experimental data are not systematic but are particular to individual configurations and can be attributed to changes in flow interference effects, particularly when flaps are deployed, or to small regions of separated flow occurring as the angle of attack and lift coefficient increase. Sketch 3.1 shows a typical example of predicted and experimental values, plotted against lift coefficient, for an aircraft in both the cruise configuration and the landing configuration. Changes in wing aspect ratio and sweep, body size and tail assembly serve only to alter the overall magnitudes of Y_v and N_v and, subject to the preceding remarks on the particular characteristics of individual aircraft, they do not alter the variation with lift coefficient.

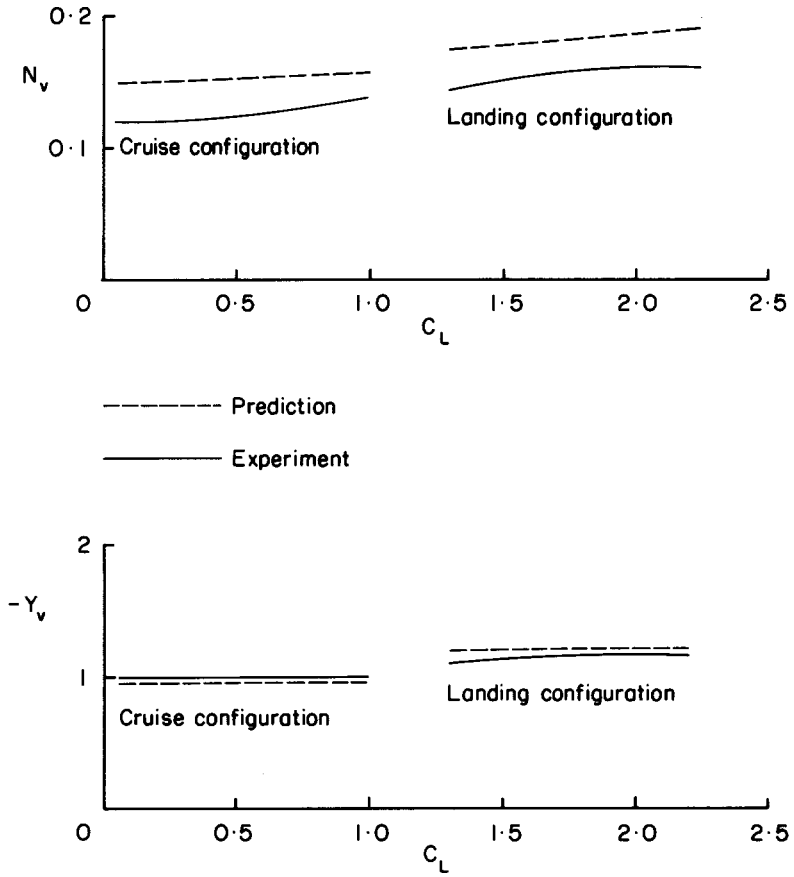

Sketch 3.1 Comparison of typical predicted and experimental variations with lift coefficient

3.2 Overall Accuracy

In general, for both cruise and flaps-deployed configurations, Y_v is predicted to within about ± 0.1 and N_v to within about ± 0.04. These levels of accuracy are consistent with those to which the individual components of Y_v and N_v are predicted, although in the case of N_v the overall errors in prediction can be a significant proportion of the total derivative. This is a consequence of the fact that the total value of N_v is primarily the resultant of the destabilising wing-body component and the stabilising fin component (the nacelle and flap contributions being comparatively small). The magnitudes of each of these components exceeds the magnitude of the resultant and thus any error in predicting the individual components increases in importance in terms of the overall accuracy. (This is well illustrated by Sketch 5.4 in the Example.) Sketch 3.2 summarises the overall levels of agreement between the predicted and experimental values of Y_v and N_v, with each configuration studied being represented in the cruise or the landing configuration by a single point taken at an appropriate value of lift coefficient. There is no difference in the overall accuracy of prediction between the low-speed wind-tunnel test data and the (less numerous) data obtained from tests at high-subsonic speeds.

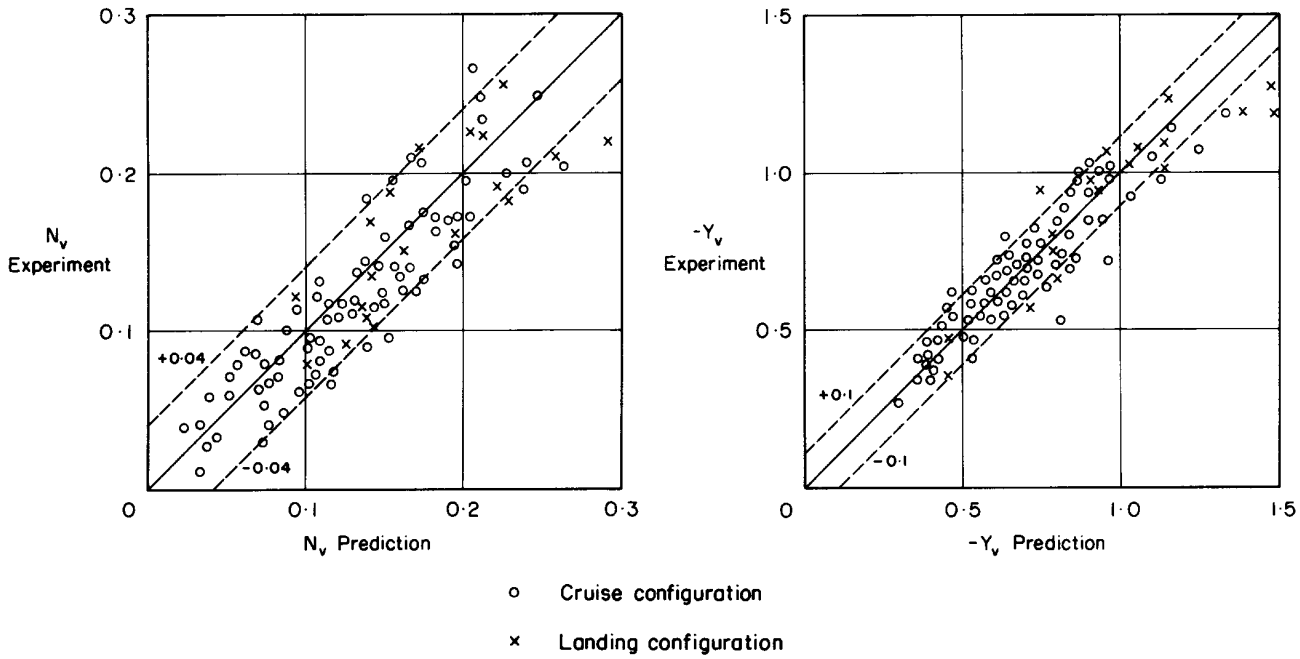

Sketch 3.2 Comparison of experimental and predicted total values

3.2.1 Wing-body contribution

Examination of part-model test data has shown that the wing-body contribution to Y_v and N_v is usually quite well estimated by the method in Item No. 79006 but that the predicted values tend to decrease in reliability if the centre of gravity position is a long way from the body mid-point. This is due to a tendency to overestimate the magnitude of the assumed variation of N_v with the centre of gravity position which, in some cases, results in too large a departure from the value of N_v appropriate to a mid-body centre of gravity position (see Section 5.2 of the Example). However, the overestimate is only significant when the variation due to the centre of gravity position is large and it should be noted that the method in Item No. 79006 was developed only to cater for small changes in N_v. The method should therefore only be used with caution if predicted variations are in excess of 0.03, or if the centre of gravity position is well away from the body mid-point, $(l - 0.5l_b) \geq 0.1l_b$. (Variations greater than 0.03 are, for example, sometimes predicted for small wing-span aircraft with centre of gravity positions well to the rear of the body mid-point.)

Part-model data for bodies with non-circular cross-sections have confirmed that the body cross-section shape has an important effect on the wing-body contribution, as discussed in Item No. 79006. (The effect of cross-section shape on the other components is negligible and, where necessary, a mean value can be taken for the body diameter.) Item No. 79006 contains a table giving examples of typical correction factors for converting the wing-body components of Y_v and N_v from values appropriate to circular cross-sections to values appropriate to non-circular cross-sections. The data studied have shown that the use of correction factors deduced from this table results in an overall improvement in the accuracy of prediction of the total values of Y_v and N_v for some fighter and light and general aviation aircraft with non-circular cross-sections. It should, however, be remembered that the factors in the table are intended only to show the sort of changes that can occur, being based on a small number of data, and for most practical configurations the selection of a correction factor is not an exact process and can only be made as an approximation after comparing the actual configuration of interest with the examples given in Item No. 79006.

Item No. 79006 also points out that there is a theoretical wing-planform contribution to Y_v and N_v, which increases with wing sweepback and is proportional to C_L^2, but which is usually small enough to be neglected. The data that have been studied confirm that the planform contribution is unimportant, with the experimental data showing little or no increase with C_L of the kind that would be consistent with the theoretical prediction.

3.2.2 Fin contribution

Examination of part-model wind-tunnel data has indicated that the method in Item No. 82010 provides a generally satisfactory estimate of the contribution of a conventional tail assembly to Y_v and N_v. The method predicts the effect of adding a fin, allowing for the presence of the body, the tailplane and the wing, and in particular includes the load induced on the body by the fin and tailplane. The user is, however, reminded that the method assumes that the tailplane contributes to the lateral effectiveness only through its interference effects with the fin and the body. The wind-tunnel data for complete models confirm that there is no other significant contribution to Y_v and N_v arising directly from the tailplane, with the possible exception of cases where the tailplane is body-mounted and has large angles ($\sim 15°$) of dihedral or anhedral. For such configurations comparison of the total experimental and predicted values suggests that, compared to an otherwise similar tail assembly with a horizontal tailplane, the presence of tailplane dihedral can cause a small reduction (~ 5 to 10 per cent) in the contribution of the tail assembly, whereas the presence of tailplane anhedral can increase the contribution by a similar amount. The user's attention is drawn to this, but the small size of the effect, the difficulty of isolating it reliably from data on complete models, and the general absence of data for tests in which tailplane angles are varied systematically, all prevent any recommendation of a general correction procedure for the fin contribution predicted by Item No. 82010. In the case of anhedral angles the deduction of any correction procedure is especially difficult since most data for such tailplanes are for fighter-type aircraft, which frequently have non-circular body cross-sections, making it harder to isolate any effect of the tailplane because of the increased uncertainty in the prediction of the wing-body component (see Section 3.2.1).

3.2.3 Flap contribution

The experimental data studied have shown that the flap contribution to Y_v and N_v is estimated quite well by using the method in Item No. 81013 in conjunction with theoretical estimates of the increments in lift and viscous drag coefficients due to flap deployment. The Data Items which predict flap lift and drag coefficients usually provide sufficiently accurate estimates in the case of lift increments but they are more limited in their coverage of flap types for drag increments, with no data for multi-slotted flap systems or systems where there is a large translation of the flap. Therefore, in such cases it is necessary to use other sources of data, such as Reference 46. As the flap contribution is largest for configurations with tailplanes mounted on the fin, when it is the flap lift coefficient that is important, this limitation does not place too great a restriction on the calculation.

4. DERIVATION AND REFERENCES

4.1 Derivation

The Derivation lists selected sources that have assisted in the preparation of this Item.

ESDU Items

1. ESDU — Conversion factor for profile drag increment for part-span flaps. Item No. Aero F.02.01.07, Engineering Sciences Data Unit, London, June 1944.
2. ESDU — Profile drag coefficient increment due to full-span single-slotted flaps (Handley Page and NACA types). Item No. Aero F.02.01.06, Engineering Sciences Data Unit, London, November 1944.
3. ESDU — Information on the use of Data Items on yawing moment derivatives of an aeroplane. Item No. Aero A.07.01.00, Engineering Sciences Data Unit, London, November 1946.
4. ESDU — Lift coefficient increment due to full-span double flap (main flap slotted). Item No. Aero F.01.01.09, Engineering Sciences Data Unit, London, December 1948.
5. ESDU — Lift coefficient increment due to full-span slotted flaps. Item No. Aero F.01.01.08, Engineering Sciences Data Unit, London, March 1949.
6. ESDU — Lift-curve slope of swept and tapered wings. Item No. Aero W.01.01.01, Engineering Sciences Data Unit, London, March 1953.
7. ESDU — Slope of lift curve for two-dimensional flow. Item No. Aero W.01.01.05, Engineering Sciences Data Unit, London, January 1955.
8. ESDU — Lift-curve slope for single fin and rudder. (i) Body shape merging into fin. Item No. Aero C.01.01.01, Engineering Sciences Data Unit, London, January 1955.
9. ESDU — Lift-curve slope for twin fins and rudders. Item No. Aero C.01.01.02, Engineering Sciences Data Unit, London, March 1955. (Superseded by Item No. 92007.)
10. ESDU — Subsonic lift-dependent drag due to boundary layer of plane, symmetrical section wings. Item No. 66032, Engineering Sciences Data Unit, London, November 1966.
11. ESDU — Lift-curve slope and aerodynamic centre position of wings in inviscid subsonic flow. Item No. 70011, Engineering Sciences Data Unit, London, July 1970.
12. ESDU — Lift coefficient increment at low speeds due to full-span split flaps. Item No. 74009, Engineering Sciences Data Unit, London, May 1974.
13. ESDU — Low-speed drag coefficient increment at zero lift due to full-span split flaps. Item No. 74010, Engineering Sciences Data Unit, London, July 1974.

14. ESDU — Rate of change of lift coefficient with control deflection for full-span plain controls. Item No. 74011, Engineering Sciences Data Unit, London, July 1974.

15. ESDU — Conversion of lift coefficient increment due to flaps from full span to part span. Item No. 74012, Engineering Sciences Data Unit, London, July 1974.

16. ESDU — Information on the use of Data Items on flaps including estimation of the effects of fuselage interference. Item No. 75013, Engineering Sciences Data Unit, London, July 1975. (Superseded by Item Nos 97002 and 97003.)

17. ESDU — Geometric properties of cranked and straight-tapered wing planforms. Item No. 76003, Engineering Sciences Data Unit, London, January 1976.

18. ESDU — Wing-body yawing moment and sideforce derivatives due to sideslip: N_v and Y_v (With Addendum A on nacelle effects). Item No. 79006, Engineering Sciences Data Unit, London, June 1979.

19. ESDU — Effect of trailing-edge flaps on sideforce and yawing moment derivatives due to sideslip, $(Y_v)_f$ and $(N_v)_f$. Item No. 81013, Engineering Sciences Data Unit, London, June 1981.

20. ESDU — Contribution of fin to sideforce, yawing moment and rolling moment derivatives due to sideslip, $(Y_v)_F$, $(N_v)_F$, $(L_v)_F$, in the presence of body, wing and tailplane. Item No. 82010, Engineering Sciences Data Unit, London, April 1982.

Wind-tunnel Data

21. TAMBURELLO, V. WEIL, J. — Wind-tunnel investigation of the effect of power and flaps on the static lateral characteristics of a single-engine low-wing airplane model. NACA tech. Note 1327, 1946.

22. KIRBY, D.A. — Low speed tunnel tests on a 1/5th scale model of a single-jet fighter with a 40° sweptback wing. RAE Rep. aero 2382, 1950.

23. GOODMAN, A. — Effects of wing position and horizontal-tail position on the static stability characteristics of models with unswept and 45° sweptback surfaces with some reference to mutual interference. NACA tech. Note 2504, 1951.

24. GRAHAM, D. KOENIG, D.G. — Tests in the Ames 40- by 80-foot wind tunnel of an airplane configuration with an aspect ratio 2 triangular wing and an all-movable horizontal tail – lateral characteristics. NACA RM A51L03 (TIL 4280), 1952.

25. GRINER, R.F. — Static lateral stability characteristics of an airplane model having a 47.7° sweptback wing of aspect ratio 6 and the contribution of various model components at a Reynolds number of 4.45×10^6. NACA RM L53G09 (TIL 3885), 1953.

26. GOODMAN, A. THOMAS, D.F. — Effects of wing position and fuselage size on the low-speed static and rolling stability characteristics of a delta wing model. NACA tech. Note 3063, 1953.

27. WETZEL, B.E. — Wind-tunnel investigation at subsonic and supersonic speeds of a fighter model employing a low-aspect-ratio unswept wing and a horizontal tail mounted well above the wing plane – lateral and directional stability. NACA RM A54H26 b (TIL 6638), 1954.

28. WOLHART, W.D. THOMAS, D.F. — Static longitudinal and lateral stability characteristics at low speed of unswept-midwing models having wings with an aspect ratio of 2, 4 or 6. NACA tech. Note 3649, 1955.

29. LETKO, W. WILLIAMS, J.L. — Experimental investigation at low speed of effects of fuselage cross section on static longitudinal and lateral stability characteristics of models having 0° and 45° sweptback surfaces. NACA tech. Note 3551, 1955.

30. HALLISSY, J.M. — Transonic wind-tunnel measurements of static lateral and directional stability and vertical tail loads for a model with a 45° sweptback wing. NACA RM L55L19 (TIL 6683), 1955.

31. SILVERS, H.N. KING, T.J. — Investigation at high subsonic speeds of the effect of horizontal-tail location on longitudinal and lateral stability characteristics of a complete model having a sweptback wing in a high location. NACA RM L56B10 (TIL 5071), 1956.

32. ARABIAN, D.D. — Effect of large negative dihedral of the horizontal tail on longitudinal and lateral stability characteristics of a swept-wing configuration at transonic speeds. NACA RM L55I20 (TIL 6024), 1956.

33. WOLHART, W.D. THOMAS, D.F. — Static longitudinal and lateral stability characteristics at low speed of 45° sweptback-midwing models having wings with an aspect ratio of 2, 4 or 6. NACA tech. Note 4077, 1957.

34. WOLHART, W.D. THOMAS, D.F. — Static longitudinal and lateral stability characteristics at low speed of 60° sweptback-midwing models having wings with an aspect ratio of 2, 4 or 6. NACA tech. Note 4397, 1958.

35. FOURNIER, P.G. — Low-speed investigation of static longitudinal and lateral stability characteristics of an airplane configuration with a highly tapered wing and with several body and tail arrangements. NASA tech. Note D-217, 1960.

36. CHAMBERS, J.R. ANGLIN, E.L. — Analysis of lateral-directional stability characteristics of a twin-jet fighter airplane at high angles of attack. NASA tech. Note D-5361, 1969.

37. SHIVERS, J.P. FINK, M.P. WARE, G,M. — Full-scale wind-tunnel investigation of the static longitudinal and lateral characteristics of a light single-engine low-wing airplane. NASA tech. Note D-5857, 1970.

38. FINK, M.P. FREEMAN, D.C. GREER, H.D. — Full-scale wind-tunnel investigation of the static longitudinal and lateral characteristics of a light single-engine airplane. NASA tech. Note D-5700, 1970.

39. FLETCHER, H.S. — Comparison of several methods for estimating low-speed stability derivatives for two airplane configurations. NASA tech. Note D-6531, 1971.

40. FINK, M.P. SHIVERS, J.P. GREER, H.D. — The effects of configuration changes on the aerodynamic characteristics of a full-scale mockup of a light twin-engine airplane. NASA tech. Note D-6896, 1972.

41. MARGASON, R.J. VOGLER, R.D. WINSTON, M.M. — Wind-tunnel investigation at low speeds of a model of the Kestrel (XV-6A) vectored-thrust V/STOL airplane. NASA tech. Note D-6826, 1972.

42. GREER, H.D. SHIVERS, J.P. FINK, M.P. CARTER, C.R. — Wind-tunnel investigation of static longitudinal and lateral characteristics of a full-scale mockup of a light single-engine high-wing airplane. NASA tech. Note D-7149, 1973.

43. GRAFTON, S.B. CHAMBERS, J.R. COE, P.L. — Wind-tunnel free-flight investigation of a model of a spin-resistant fighter configuration. NASA tech. Note D-7716, 1974.

44. BAe — Unpublished wind-tunnel data from British Aerospace, Aircraft Group, Hatfield-Chester, Manchester, Warton and Weybridge-Bristol Divisions.

45. SAAB-SCANIA — Unpublished wind-tunnel data. Saab-Scania, Sweden.

4.2 References

The References are recommended sources of information supplementary to that in this Item.

46. YOUNG, A.D. — The aerodynamic characteristics of flaps. ARC R & M 2622, 1953.

Issued after Item No. 82011

47. ESDU — Low-speed drag coefficient increment at constant lift due to full-span plain flaps. ESDU International. Item No. 87024, 1987.

5. EXAMPLE

This Section provides a worked example to show how Y_v and N_v are calculated for the aircraft dimensioned as shown in Sketches 5.1 and 5.2, together with the additional geometric information in Table 5.1. Both inner and outer flaps are of the single-slotted type. The longitudinal body axis is taken parallel to the mid-body centre-line and passes through the aircraft's centre of gravity position. Angles of attack are expressed in terms of this axis.

Calculations are performed for two flight conditions,

(i) a cruise condition with $\alpha = 0$, Mach number = 0.78 and Reynolds number/metre = $7.5 \times 10^6\,\mathrm{m}^{-1}$,

and

(ii) a landing condition with $\alpha = 6$, Mach number = 0.2 and Reynolds number/metre = $4.5 \times 10^6\,\mathrm{m}^{-1}$.

Where appropriate the components of N_v are also expressed as functions of α. The variation of the total values of Y_v and N_v with angle of attack and lift coefficient are illustrated by sketches.

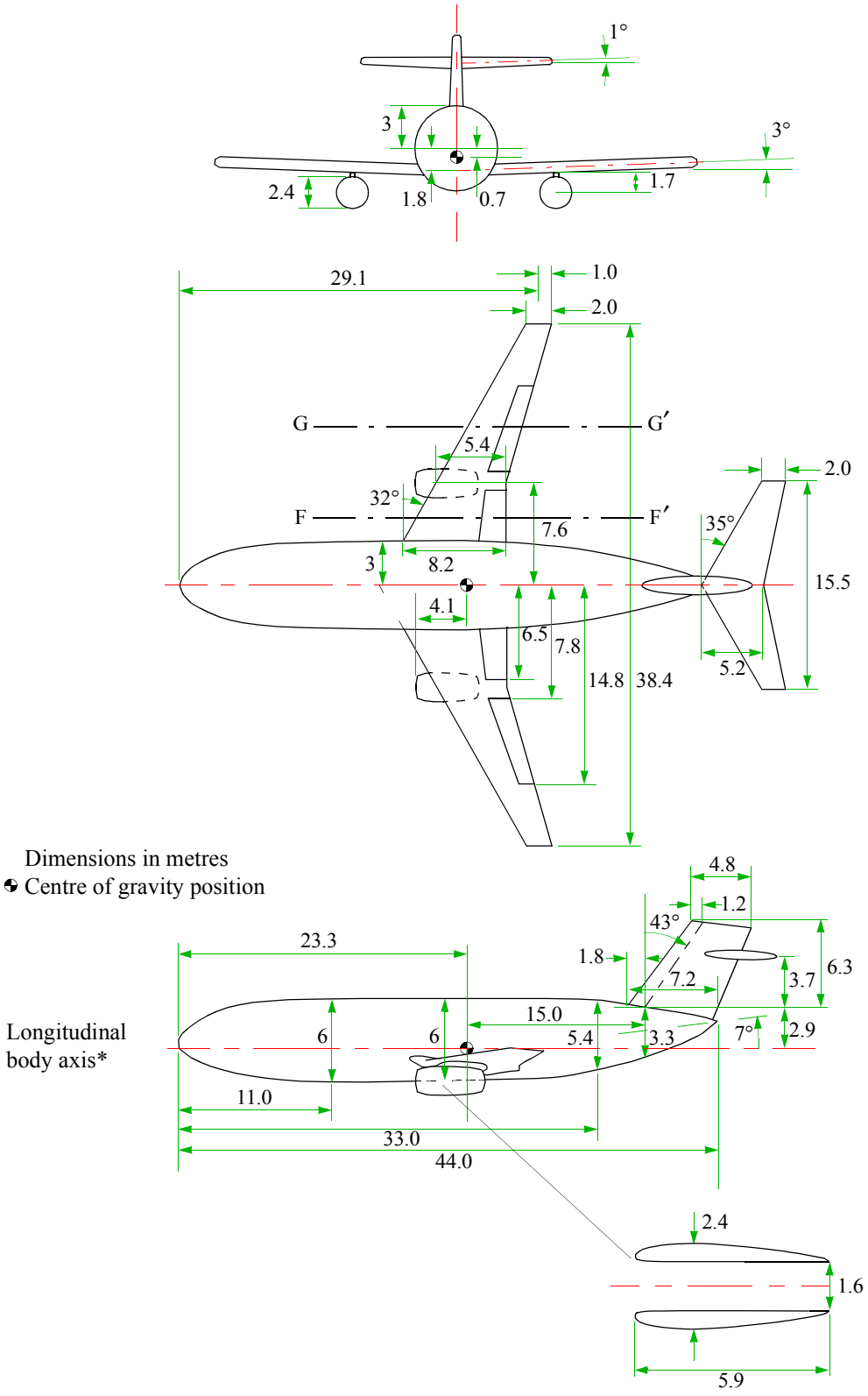

Sketch 5.1 Aircraft geometry

* The longitudinal body axis is a reference axis, fixed in the body in the plane of symmetry and passing through the centre of gravity position. The exact direction of the axis in the plane of symmetry is conventionally determined by considerations of mid-body geometry, the axis being taken parallel to some convenient "horizontal" datum.

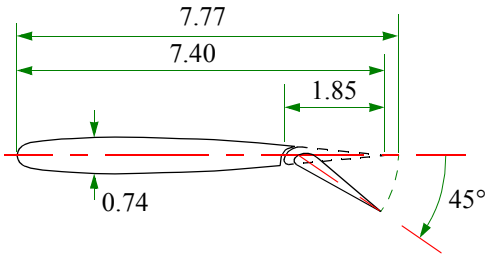

Section through FF′ in Sketch 5.1

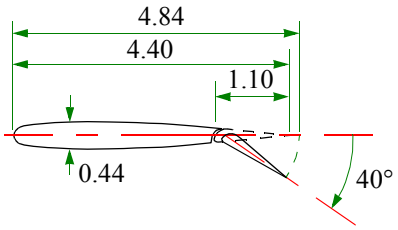

Section through GG′ in Sketch 5.1

Sketch 5.2 Section geometry of flaps

TABLE 5.1 Additional Geometric Parameters for Aircraft in Sketch 5.1

WING Angle between wing zero-lift line and longitudinal body axis Average section trailing-edge angle Average section thickness-to-chord ratio	 3° 10° 0.10	
FLAPS (single slotted) Flap-chord to wing-chord ratio Flap-chord to extended-wing-chord ratio Extended-wing-chord to wing-chord ratio Flap deflection angle	At section FF′ 0.250 0.238 1.05 45°	At section GG′ 0.250 0.227 1.10 40°
BODY Maximum cross-sectional area Side elevation area	 28.3 m^2 224.0 m^2	
FIN Side area between tip and root chords	 37.8 m^2	
Note (i) The wing and flap section parameters are taken in planes parallel to the aircraft plane of symmetry. (ii) Boundary-layer transition is assumed to occur at the leading-edge of the wing.		

5.1 Calculation of Wing Planform Parameters

See Item No. 76003 for Notation.

Before commencing the estimation of Y_v and N_v it is usually necessary to calculate a number of geometric parameters for the wing planform which are not immediately available from Sketches 5.1, 5.2 or Table 5.1. This is because, apart from the Item for estimating the flap contribution, the Items involved in the calculation of Y_v and N_v (and also those involved in the calculation of the corresponding rolling moment derivative) apply directly only to straight-tapered wings. Therefore, unless the aircraft has this type of wing, for which the planform parameters can be readily obtained from a scale diagram, a straight-tapered wing equivalent to the true wing has to be constructed by the method in the Addendum to Item No. 76003, Derivation 17. That Item represents a cranked wing by a straight-tapered wing which has the same span, the same tip chord and the same exposed wing area outside the intersection of the wing and body planforms as the true wing. The equivalent-wing planform parameters which result from applying the method in item No. 76003 to the aircraft in Sketch 5.1 are summarised in Table 5.2.

TABLE 5.2 Properties of Equivalent Straight-tapered Wing Planform

Parameter	*Value*	*Parameter*	*Value*
Wing area, S	194.3 m^2	Leading-edge sweep, Λ_0	32.0°
Aspect ratio, A	7.59	Quarter-chord sweep, $\Lambda_{¼}$	28.6°
Aerodynamic mean chord, $\bar{\bar{c}}$	5.68 m	Half-chord sweep, $\Lambda_{½}$	25.0°
Ratio of tip chord to root chord, λ	0.246		

5.2 Calculation of Wing-body Contribution, $(Y_v)_{WB}$ and $(N_v)_{WB}$

See Item No. 79006 for Notation.

In Item No. 79006 the wing-body contribution to the yawing moment derivative is given as an empirical equation and presented in graphical form as a function of the body geometric parameters l_b^2/S_b and h_1/h_2, for a yaw axis passing through the middle of the body. This is written as $(N_{v\,mid})_{WB}$ *. Calculation of the yawing moment contribution for a general axis position is obtained by adding the moment produced by the product of the sideforce derivative $(Y_v)_{WB}$ and the distance between the middle of the body and the required yaw axis location, so that $(N_v)_{WB} = (N_{v\,mid})_{WB} + (l - 0.5l_b)(Y_v)_{WB}/b$. The sideforce derivative is given as an empirical equation. It comprises a body term, a wing-body interference term and a wing dihedral term and is written

$$-(Y_v)_{WB} = [0.0714 + 0.674h^2/S_b + hbFF_W(4.95|z|/h - 0.12)/S_b]S_b/S + 0.006|\Gamma|.$$

The two factors F and F_W which are involved in the wing-body interference term are given graphically in Item No. 79006 as functions of the wing-body geometric parameters b/d, $|z/h|$, A and λ. The values of the quantities involved in the calculation of $(Y_v)_{WB}$ and $(N_v)_{WB}$ for the aircraft geometry in Sketch 5.1 are set out in Table 5.3, with the equivalent-wing values of A and λ being used. The components $(Y_v)_{WB}$ and $(N_v)_{WB}$ are independent of α.

See comments in Section 3.2.1 on effect of centre of gravity location, body cross-section shape and wing planform.

TABLE 5.3

Parameter	*Cruise and landing configuration*
l_b^2/S_b	8.64
h_1/h_2	1.11
$-(N_{v\,mid})_{WB}Sb/S_bl_b$	0.116
$(N_{v\,mid})_{WB}$	– 0.153
h^2/S_b	0.161
hb/S_b	1.029
b/d	6.4
$\|z\|/h$	0.3
F	0.078
A	7.59
λ	0.246
F_W	0.99
Γ	3°
$(Y_v)_{WB}$	– 0.350
$(l - 0.5l_b)/b$	0.034
$(N_v)_{WB}$	– 0.165

* In Item No. 79006 itself the notation $(\ )_{WB}$ is omitted from Y_v and N_v.

5.3 Calculation of Nacelle Contribution, $(Y_v)_n$ and $(N_v)_n$

See Item No. 79006 for Notation.

The nacelle contribution is treated in Addendum A of Item No. 79006 for wing and rear-body mounted jet-engine nacelles. (The effect of any wing-mounted piston engine or turboprop nacelles is considered to be negligible.) The values of the quantities involved in the estimation of the effect of the wing-mounted jet-engine nacelles shown in Sketch 5.1 are given in Table 5.4. The nacelle contribution is independent of angle of attack.

TABLE 5.4

Parameter	*Cruise and landing configurations*
$w_{n\ max}^2/S$	0.0296
$(z_n + 0.5w_{n\ max})/w_{n\ max}$	1.208
$(m_0 - w_{n\ max})/b$	0.0443
$w_{n\ e}^2/S$	0.0132
l_n/b	0.154
$(Y_v)_n$ (total for the pair of nacelles)	− 0.123
$(N_v)_n$ (total for the pair of nacelles)	− 0.0105

5.4 Calculation of Fin Contribution, $(Y_v)_F$ and $(N_v)_F$

See Item No. 82010 for Notation.

The contribution of the fin (or fin and undeflected rudder), allowing for the presence of the body, wing and tailplane is given in Item No. 82010 for aircraft of the type shown in Sketch 5.1. (The data in Item No. Aero C.01.01.01, Derivation 8, may be used for aircraft where the rear body is very narrow and merges into the fin, and the data in Item No. Aero C.01.01.02, Derivation 9, may be used for configurations with twin fins at the extremities of a tailplane.) The method in Item No. 82010 first determines the fin contribution to the sideforce derivative due to sideslip, $(Y_v)_F$, and then estimates $(N_v)_F$ by associating $(Y_v)_F$ with longitudinal and vertical moment arms appropriate to the centre of pressure position of the fin sideforce. The value of $(Y_v)_F$ is obtained by using Item No. 70011 to estimate a basic lift-curve slope for the fin by treating it as one half of a straight-tapered wing, and then applying three correction factors to allow for the interference effects of the body, wing and tailplane. The moment arms of the centre of pressure position in directions parallel and perpendicular to the longitudinal body axis are written $(m_F + 0.7\bar{z}_F \tan\Lambda_{¼F})$ and $(z_{crF} + 0.85\bar{z}_F)$. The parameters m_F and z_{crF} define the distance between the centre of gravity position and the point at which the fin quarter-chord line intersects the body. The value of $\bar{z}_F$ depends on the loading distribution over the fin and is a function of tailplane position. The constants 0.7 and 0.85 are empirical correction factors.

The fin contribution $(N_v)_F$ is equal to $(Y_v)_F\,[(m_F + 0.7\bar{z}_F \tan\Lambda_{¼F})\cos\alpha + (z_{crF} + 0.85\bar{z}_F)\sin\alpha]/b$. The values of the quantities resulting from the application of the method in Item No. 82010 are given in Table 5.5. Although $(N_v)_F$ is dependent on the angle of attack the variation is small for practical centre of gravity positions and values of α, being typically about 0.01 as α increases from 0 to 10°.

See comments in Section 3.2.2 on effect of tailplane dihedral and anhedral.

TABLE 5.5

Parameter	*Cruise configuration*	*Landing configuration*
M	0.78	0.2
α	0	6°
$(Y_v)_F$	– 0.674	– 0.603
m_F	15.0 m	15.0 m
z_{crF}	2.9 m	2.9 m
$\bar{z}_F/h_F$	0.49	0.49
h_f	6.3 m	6.3 m
b	38.4 m	38.4 m
$\Lambda_{¼F}$	43°	43°
$(N_v)_F$	0.299	0.275
$(N_v)_F$ (as a function of α)	$0.674(0.443\cos\alpha + 0.144\sin\alpha)$	$0.603(0.443\cos\alpha + 0.144\sin\alpha)$

5.5 Calculation of Trailing-edge Flap Contribution, $(Y_v)_f$ and $(N_v)_f$

See Item No. 81013 for Notation.

The flap contribution is treated in Item No. 81013 in terms of a number of separate components, namely a wing aspect ratio component, a wing sweepback component, a fin-tailplane component and a wing-body interference component. These components are denoted by square brackets $[\ ]_A$, $[\ ]_\Lambda$, $[\ ]_{FT}$ and $[\ ]_{WB}$. Their sizes are related to the increments in lift and viscous drag coefficients caused by flap deployment and to the positions of the flaps and tail assembly relative to the centre of gravity position. They are summed to give the total flap contribution.

The wing-body sideforce component $[(Y_v)_f]_{WB}$ involves an empirical factor F_1, which is given graphically as a function of the interference term $AFF_W(4.95|z|-0.12h)/b$ used in Item No. 79006 when estimating $(Y_v)_{WB}$ (see Section 5.2). The fin-tailplane components $[(Y_v)_f]_{FT}$ and $[(N_v)_f]_{FT}$ are related to the fin contribution derivatives $(Y_v)_F$ and $(N_v)_F$ estimated as described in Section 5.4, with an empirical factor F_2, which is given graphically as a function of tailplane height, allowing for interference between the flap system and the tail assembly. If the flap system consists of inner and outer segments, as in this example, the components $[(Y_v)_f]_\Lambda$, $[(Y_v)_f]_{WB}$, $[(N_v)_f]_\Lambda$ and $[(N_v)_f]_A$ are evaluated separately for the two segments, using the increments in lift and viscous drag coefficients due to flap deployment that are appropriate to the individual flap segments. (Note that $[(Y_v)_f]_A$ and $[(N_v)_f]_{WB}$ are always identically zero.)

For the single-slotted flaps that are shown in Sketches 5.1 and 5.2 Item No. Aero F.01.01.08 (Derivation 5) is used to determine, separately, the full-span value of lift coefficient increment appropriate to the flap deflection and flap-chord to wing-chord ratios of the inner and outer panels. The part-span correction method in Item No. 74012 (Derivation 15) is then applied to reduce the full-span coefficients to the values appropriate to the spanwise extent of each panel. Note that the inner panel has a fictitious inboard extension added to account theoretically for body interference, as described in Item No. 75013 (Derivation 16). These procedures give $\Delta C_{Lfa} = 0.369$ and $\Delta C_{Lfb} = 0.356$.

Similarly, Item No. Aero F.02.01.06 (Derivation 2) provides the full-span values of the viscous drag coefficient increments, at zero lift, which are appropriate to the inner and outer flap panels, with the part-span correction method in Item No. Aero F.02.01.07 (Derivation 1) being used to allow for the spanwise extent of each panel. (There is no body interference correction in this case.) The corrections to the zero-lift viscous drag coefficients to allow for the lift-dependent drag of the boundary layer are discussed in Item No. 66032 (Derivation 10) which gives values for the isolated wing, albeit derived from a database where boundary-layer transition was not fixed. In this case the corrections are negligible and the required viscous drag coefficient increments are equal to the zero-lift values. The coefficients obtained are $\Delta C'_{Dfa} = 0.014$ and $\Delta C'_{Dfb} = 0.014$.

Table 5.6 sets out the quantities involved in calculating $(Y_v)_f$ and $(N_v)_f$. The value of $(N_v)_f$ depends on the angle of attack because it is related to the contribution $(N_v)_F$, but the variation with α is usually small. The flap contribution will also reflect any variation with α of the flap lift and viscous drag coefficient increments such as can occur with flap systems which extend the local wing chord, but these are also small. The combination of these variations with α leads to an increase in the flap contribution as α increases. For a variation of α between 0 and 10° there may be, typically, an increase of 0.01 to 0.02 in the predicted value of $(N_v)_f$.

The user should note that for flaps other than those of the single-slotted type considered in this example, data on full-span lift coefficient increments may be obtained from Item No. Aero F.01.01.09 (Derivation 4) if the main flap has a second slot, from Item No. 74009 (Derivation 12) for split flaps, and from Item No. 74011 (Derivation 13) for plain flaps. The full-span drag coefficient increment for split flaps may be obtained from Item No. 74010 (Derivation 11) and from Item No. 87024 (Reference 47) for

plain flaps. For flap systems not covered by the Data Items other sources of data, such as Reference 46, may be used. The estimation of the changes in lift and viscous drag coefficients may also be influenced by the user's experience in the operation of particular flap types and any relevant experimental data.

TABLE 5.6

Parameter	*Landing configuration*		
$AFF_W(4.95\|z\|-0.12h)/b$	0.125		
F_1	0.013		
z_T/h_F	0.587		
F_2	0.085 radian		
$(Y_v)_F$	-0.603		
$(N_v)_F$	0.275		
$(N_v)_F$ (as a function of α)	$0.603(0.443\cos\alpha+0.144\sin\alpha)$		
	Inner flaps	*Outer flaps*	*Total value*
$\Delta C'_{Df}$	$\Delta C'_{Dfa}=0.014$	$\Delta C'_{Dfb}=0.014$	$\Delta C'_{Df}=0.028$
ΔC_{Lf}	$\Delta C_{Lfa}=0.366$	$\Delta C_{Lfb}=0.377$	$\Delta C_{Lf}=0.743$
l_h/b	$l_{ha}/b=0.023$	$l_{hb}/b=-0.011$	
$\bar{m}/b=(s_o+s_i)/2b$	$\bar{m}_a/b=0.124$	$\bar{m}_b/b=0.294$	
Λ_h	$\Lambda_{ha}=10°$	$\Lambda_{hb}=18.5°$	
$[(Y_v)_f]_\Lambda(=-\Delta C'_{Df})$	-0.014	-0.014	-0.028
$[(Y_v)_f]_{WB}(=-F_1\Delta C_{Lf})$	-0.0048	-0.0049	-0.0097
$[(N_v)_f]_\Lambda(=(l_h+3\bar{m}\tan\Lambda_h)\Delta C'_{Df}/b)$	0.0012	0.0039	0.0051
$[(N_v)_f]_A(=\bar{m}\Delta C'_{Df}/b)$	0.0017	0.0041	0.0058
$[(Y_v)_f]_{FT}(=(Y_v)_F F_2\Delta C_{Lf})$	-0.038		
$[(N_v)_f]_{FT}(=(N_v)_F F_2\Delta C_{Lf})$	0.0174		
$[(N_v)_f]_{FT}$ (as a function of α)*	$0.038(0.443\cos\alpha+0.144\sin\alpha)$		
$(Y_v)_f$ Total value	-0.0757		
$(N_v)_f$ Total value	0.0278		
$(N_v)_f$ Total value (as a function of α)*	$0.0109+0.038(0.443\cos\alpha+0.144\sin\alpha)$		

* In the present calculation the value of ΔC_{Lf} appropriate to $\alpha=0$ is assumed to apply to all angles of attack between 0 and 10°. Because the flap system extends the local wing chord there should be a variation in ΔC_{Lf} that is proportional to the chord extension and the wing lift coefficient (see Item No. Aero F.01.01.08, Derivation 5). The inclusion of this variation would give $\Delta C_{Lfa}=0.385$, $\Delta C_{Lfb}=0.403$ and $\Delta C_{Lf}=0.787$ at $\alpha=10°$. The components $[(Y_v)_f]_{WB}$, $[(Y_v)_f]_{FT}$ and $[(N_v)_f]_{FT}$ should, strictly, include this variation as they are directly proportional to ΔC_{Lf}. For the present calculation these variations are, however, sufficiently small to be neglected.

5.6 Total values of Y_v and N_v

The results of the preceding Sections of the example are summarised in Table 5.7, and shown as histograms in Sketches 5.3 and 5.4. Sketches 5.5 and 5.6 show the variation of the total values with α and C_L.

In Sketches 5.5 and 5.6 the values of C_L represent the total aircraft lift and are obtained from the lift-curve slope of the equivalent wing and the increment in lift coefficient due to trailing-edge flap deployment (assumed constant with α for simplicity). No contribution is estimated for the tailplane since its contribution to the overall lift coefficient is sufficiently small to be neglected for the purposes of the present comparisons. The minor contributions to the overall lift coefficient which arise from the aircraft body and the nacelles are similarly neglected, Consequently, for the cruise configuration

$$C_L = \frac{\mathrm{d}C_L}{\mathrm{d}\alpha}(\alpha + \alpha_w) = \frac{5.69}{57.3}(\alpha + 3)\,, \tag{5.1}$$

and for the landing configuration

$$C_L = \frac{\mathrm{d}C_L}{\mathrm{d}\alpha}(\alpha + \alpha_w) + \Delta C_{Lf} = \frac{4.48}{57.3}(\alpha + 3) + 0.743\,. \tag{5.2}$$

TABLE 5.7

Parameter	*Cruise configuration* ($\alpha = 0$)	*Landing configuration* ($\alpha = 6°$)
$(Y_v)_{WB}$ $(Y_v)_n$ $(Y_v)_F$ $(Y_v)_f$	– 0.350 – 0.123 – 0.674 –	– 0.350 – 0.123 – 0.603 – 0.076
Total Y_v	–1.147	–1.152
$(N_v)_{WB}$ $(N_v)_n$ $(N_v)_F$ $(N_v)_f$	– 0.165 – 0.014 + 0.299 –	–0.165 – 0.011 + 0.275 + 0.028
Total N_v	+ 0.123	+ 0.127

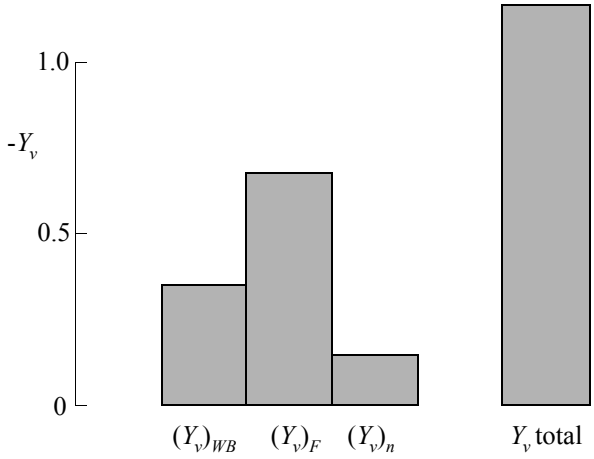

Cruise configuration $\alpha = 0$

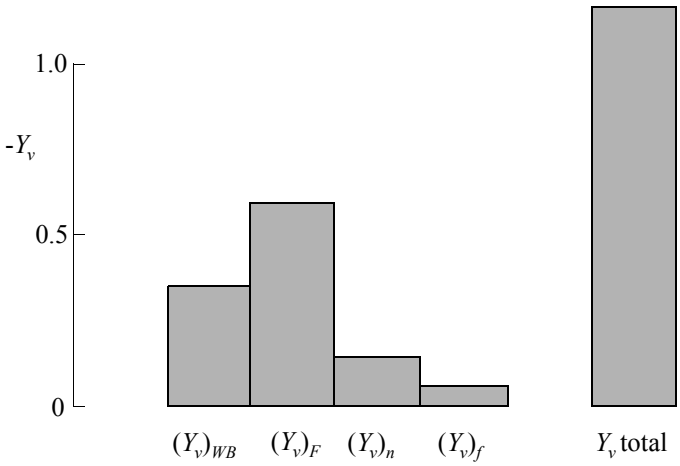

Landing configuration $\alpha = 6°$

Sketch 5.3 Comparison of components of Y_v

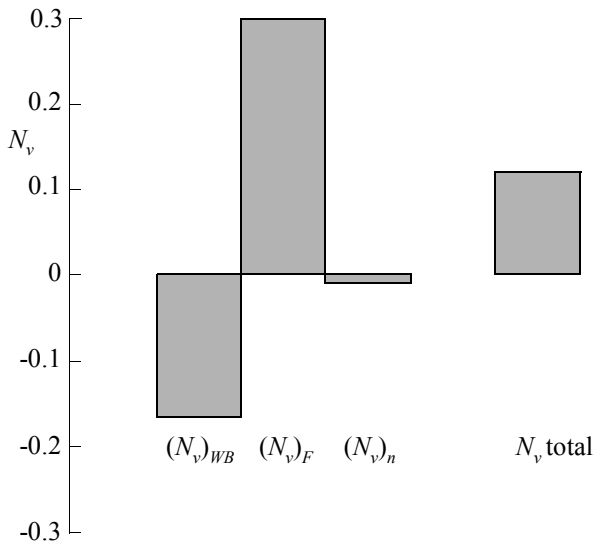

Cruise configuration $\alpha = 0$

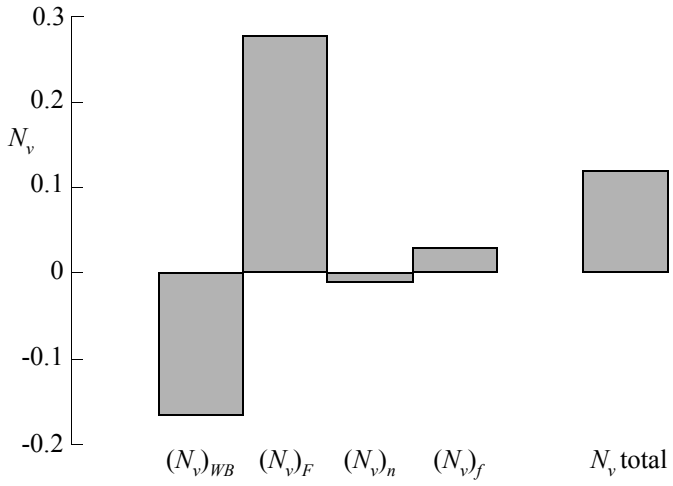

Landing configuration $\alpha = 6°$

Sketch 5.4 Comparison of components of N_v

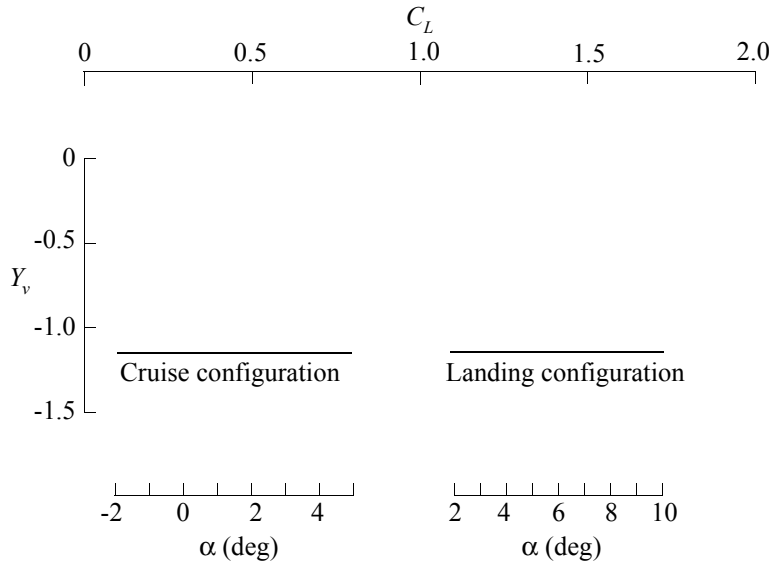

Sketch 5.5 Variation of total Y_v with C_L and α

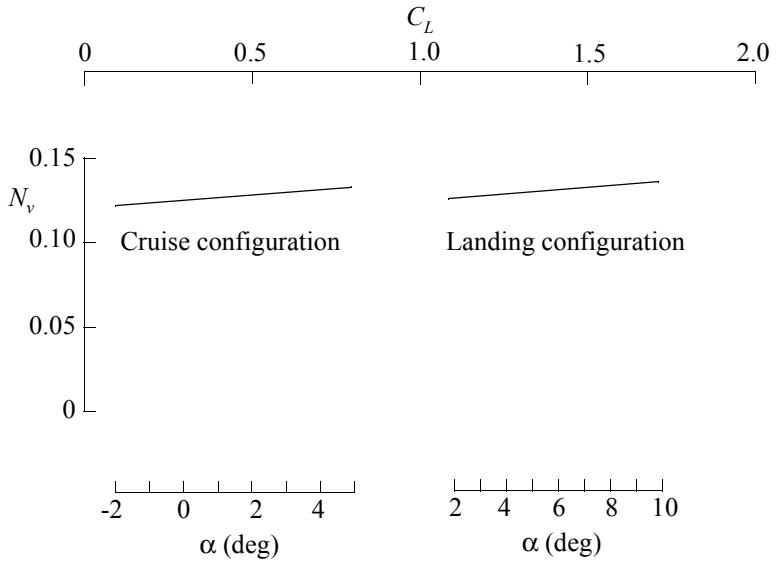

Sketch 5.6 Variation of total N_v with C_L and α

THE PREPARATION OF THIS DATA ITEM

The work on this particular Item was monitored and guided by the Aerodynamics Committee which first met in 1942 and now has the following membership:

Chairman

Mr P.K. Jones – British Aerospace, Manchester Division

Vice-Chairman

Mr J. Weir – Salford University

Members

Mr D. Bonenfant – Aérospatiale, Toulouse, France
Mr E.A. Boyd – Cranfield Institute of Technology
Mr K. Burgin – Southampton University
Mr E.C. Carter – Aircraft Research Association
Mr J.R.J. Dovey – British Aerospace, Warton Division
Dr J.W. Flower – Bristol University
Mr H.C. Garner – Royal Aircraft Establishment
Mr A. Hipp – British Aerospace, Stevenage-Bristol Division
Dr B.L. Hunt* – Northrop Corporation, Hawthorne, Calif., USA
Mr J. Kloos* – Saab-Scania, Linköping, Sweden
Mr J.R.C. Pedersen – Independent
Mr I.H. Rettie* – Boeing Aerospace Company, Seattle, Wash., USA
Mr F.W. Stanhope – Rolls-Royce Ltd, Derby
Mr H. Vogel – British Aerospace, Weybridge-Bristol Division.

* Corresponding Member

The member of staff who undertook the technical work involved in the initial assessment of the available information and the construction and subsequent development of the Item was

Mr R.W. Gilbey – Senior Engineer.